

## **Phase Transformations in Oxides Above 2000 °C: Experimental Technique Development**

Sergey V. Ushakov<sup>1</sup>, Pardha S. Maram<sup>1</sup>, Denys Kapush<sup>1</sup>, Alfred J. Pavlik III<sup>1</sup>, Matthew Fyhrie<sup>1</sup>, Leighanne C. Gallington<sup>2</sup>, Chris J. Benmore<sup>2</sup>, Richard Weber<sup>2,3</sup>, Joerg C. Neuefeind<sup>4</sup>, Jake W. McMurray<sup>4</sup>, Alexandra Navrotsky<sup>1</sup>

<sup>1</sup>Peter A. Rock Thermochemistry Laboratory and NEAT ORU, University of California Davis, One Shields Avenue, Davis, CA 95616

<sup>2</sup>X-ray Science Division, Advanced Photon Source, Argonne National Laboratory, 9700 S. Cass Avenue, Lemont, IL 60439

<sup>3</sup>Materials Development, Inc., 3090 Daniels Court, Arlington Heights, IL 60004

<sup>4</sup>Chemical and Engineering Materials Division, Oak Ridge National Laboratory, Oak Ridge, TN 37831

## **Abstract**

The oxidation of boride and carbide-based ultra-high-temperature ceramics is the primary limiting factor for their use as aerodynamic surfaces. Understanding the behaviour of the oxides that can result from oxidation of metal borides and carbides at very high temperatures is essential to optimise and tailor the performance of these materials; yet experimental thermodynamic and structural data for refractory oxides above 2000°C are mostly absent. The following techniques that can be applied to fill this gap are discussed: (i) commercial ultra-high temperature differential thermal analysis for investigation of phase transformations and melting in inert environments to 2500°C, (ii) a combination of laser heating with a splittable nozzle aerodynamic levitator for splat quenching and drop calorimetry from temperatures limited only by sample evaporation, (iii) synchrotron X-ray and neutron diffraction on laser-heated aerodynamically levitated oxide samples for *in situ* observation of phase transformations in variable atmospheres, refinement of high-temperature structures and thermal expansion. Recent experimental findings include anomalous thermal expansion of the defect fluorite phase of YSZ, thermodynamics of pyrochlore-fluorite transformation from high-temperature structure refinements, and measurement of thermal expansion to the melting temperatures and fusion enthalpies of Zr, Hf, La, Yb and Lu oxides. These methods provide temperatures, enthalpies and volume change for phase transformations above 2000°C, which are required for thermodynamic assessments and calculation of phase diagrams of multicomponent systems.

## Introduction

Ultra-high-temperature ceramics (UHTC) are sought to withstand the aerodynamic heating of sharp leading edges of hypersonic rockets in the atmosphere [1]. All UHTC formulations are based on Hf and Zr carbides and borides owing to their light weight and melting temperature above 3000°C. The effect of minor UHTC components on oxidation rates, melting, and phase transformation in formed oxide is of critical concern. However, the experimental data for Zr and Hf oxide systems above 2000°C are scant and were often obtained more than 30 years ago using ad hoc built instrumentation employing graphite or tungsten furnaces restricted to reducing conditions [2].

Besides UHTC-related applications, there is another reason to study refractory oxides. Relatively few oxides melt above 2000°C, but ZrO<sub>2</sub>, HfO<sub>2</sub>, and rare earth oxides fall into this category. Their compounds are used for diverse applications ranging from ceramic implants and thermal barrier coatings to high-k dielectrics, solid electrolytes and oxygen sensors, yet their thermodynamic properties, structure, and phase transformations above 2000°C are not well studied even for pure oxides. Even though these oxides melt above 2000°C, measurements of their enthalpies and entropies of transformation and fusion are needed for modelling phase equilibria at lower temperatures in multicomponent systems.

Computational approaches, once developed, can be applied to different types of compounds with relative ease; however, this is not often the case for experimental approaches. The possibility of bulk heating of metals by electric current led to exploding wire techniques (more than 200 years in development!) [3] that provided heats of fusion and thermal expansion for most pure metals [4] in the solid and liquid state well above 2000°C up to their boiling temperatures. Availability of experimental thermodynamic data on pure metals, augmented by

results from first principles computations, led to streamlining development of new alloys using Calphad [5] and other integrated computational materials engineering (ICME) approaches [6]. The application of ICME for ceramic development is limited by the paucity of data for oxides at high temperatures. For example, five different thermodynamic models have been used for Calphad assessments of the Zr-ZrO<sub>2</sub> system [7]. However, all the models relied on a fusion enthalpy of ZrO<sub>2</sub> estimated from the phase diagrams published before 1936 [8].

Thermal analysis and calorimetry can provide missing data on temperatures, enthalpies, and entropies of phase transformation and melting, high-temperature X-ray and neutron diffraction can provide missing data on thermal expansion, the structure of high-temperature phases, volume change on transformations, and can be used for in situ phase diagram determination. In this paper, we summarise the recent developments and applications of these techniques for oxides above 2000°C. We start with a brief review of applied radiation thermometry since temperature measurement is often the primary source of uncertainty and confusion. In the domain of experimental techniques for measurements of temperature and properties above 2000°C, the ‘valley of death’ between innovation and commercialization is unusually deep and wide, and we will emphasise both the methods and instrumentation that are commercially available or under development that can be applied to study oxide systems of interest without years of development.

### **Temperature measurement above 2000°C**

Radiation thermometry is the only practical technique for measuring temperatures above 2000°C in a variable environment. In inert atmospheres, W-Re alloy thermocouples (G, C, and D) can be used to 2800°C. The limit of B-type (Pt30%Rh – Pt6%Rh) thermocouples, which can

be used in oxidising environments, is 1820°C. Radiation thermometry, including theory, practice, and instrumentation, has a long history of development [9-11], owing to its use in astrophysics and applications in steel, aluminum and glass industries for contactless measurements. Introduction of the first spectral band or “single-colour” pyrometer is attributed [9] to Le Chatelier for use in cement manufacturing. Optical single-colour pyrometers calibrated by the manufacturer to 3500°C have been commercially available since the 1950s [12]. They remain the most economical, fast, and sensitive method, albeit not the most accurate when a pyrometer has to be aimed at the sample surface rather than in the small opening of a chamber at a constant temperature, approximating black body geometry. For accurate measurements of surface temperature with a spectral band pyrometer, knowledge of emissivity is required, which in the general case depends not only on the material and wavelength, but on the surface roughness, curvature, angle of view, and temperature. Since in single-colour pyrometry temperature is derived from the absolute intensity, any absorption along the optical path by windows, vapours, or optical fibres must be taken into account. Emissivity at a given wavelength can be calculated from the reflection of external radiation flux for opaque materials. Combining a pulsed laser radiometer with a spectral band pyrometer operating at the same wavelength allows in situ measurements of emissivity and absorption. This method, patented by Exxon in 1983 [13] for use in petrochemical furnaces, was later developed into a commercially available instrument (Pyrolaser by Pyrometer Instrument Company) operating at 865 nm with a temperature range up to 3000°C.

In ‘two-colour’ or ratio pyrometry, the intensities of two spectral bands are measured and the temperature is evaluated from their ratio using the Planck equation. If emissivities and absorption through the optical path at measured bands are identical over a chosen range of

wavelengths, they cancel out, and the method becomes emissivity independent. Since the Planck function changes smoothly with wavelength, the farther apart the measured bands are, the more sensitive but the less accurate the ratio pyrometry is, since the assumption of equal emissivity and absorption on measured bands is less likely to hold. Thus, most commercial two-colour pyrometers have the option to be operated in single-colour mode and to set an ‘emissivity slope’ between measured bands.

In ‘multi-colour’ or spectropyrometers, intensities on multiple spectral bands are measured and used for temperature calculation, which overcomes many of the limitations of two-colour pyrometers. Spectropyrometers acting as multiple-ratio pyrometers with documented data processing algorithms [14, 15] have been commercially available for more than 20 years from a small US company (FAR Associates). New developments in instrumentation and data processing algorithms for emissivity and independent temperature measurements are being reported and patented – for example, the application of CMOS sensors as hightemperature three-colour 2D pyrometers [16] or spectropyrometer combined with a reflectometer [17]. It is our hope that they will soon develop into commercially available instruments.

### **Sample containment above 2000°C**

The choice of containers to study oxides at temperatures exceeding the melting temperature of Pt (1768°C) is limited. The use of higher melting oxides, graphite and nitrides is usually not feasible owing to their reactivity with oxides. Tungsten, Mo, and Re can be used for crucibles or strip heaters, with W ( $T_m$  3414°C) being the most common choice and used in the commercial differential thermal analyzer (DTA) described below. Melting refractory oxides in tungsten

crucibles restricts experiments to highly reducing conditions, and the formation of compounds may complicate results.

The self-crucible technique involves melting part of the sample with the rest of the sample acting as the container. This method was first used by Coutures and colleagues in 1972 [18] to measure the melting and phase transformation temperatures for rare earth oxides. Their unique experimental setup included an open rotating crucible with a 10–40 g sample load heated by focused solar radiation. Cooling traces were recorded by aiming a spectral band pyrometer into the vortex formed by the melt rotation. Currently, the self-crucible method is employed by Manara et al. [19,20] for measurement of the melting temperatures of refractory oxides and carbides with pulsed laser heating and an advanced custom spectropycrometer setup. This arrangement allows pressurising the system if needed.

Containerless techniques have been in active use and development for high-temperature studies of liquids for more than 40 years [21]. Aerodynamic levitation of laser-heated solids in gas jets was demonstrated in 1982 [22] and adapted to study melts by nuclear magnetic resonance (NMR) and by diffraction on a synchrotron source in 1997 [23]. A levitation sample holder for NMR with laser heating was patented [24] by Bruker, and an aerodynamic conical nozzle levitator with laser heating is commercially available from Materials Development, Inc. The maximum diameter of the levitated liquid oxide spheroids is limited by the surface tension of the melt and gravity, and is typically 2–4 mm. Aerodynamic levitators are currently operated in several academic and national laboratories around the world [25] and are available for high-temperature X-ray diffraction (XRD) at the 6-ID-D beamline at the Advanced Photon Source (APS) at Argonne National Laboratory in the United States, at SPRING-8 in Japan, and for neutron diffraction on the NOMAD instrument at the Spallation Neutron Source (SNS) at Oak

Ridge National Laboratory. Hennet et al. [26] developed a dual-beam heating setup where the second laser beam is focused on the bottom of the bead through the levitation orifice that they successfully operated at European synchrotron and neutron sources [27].

It must be noted that some important refractory oxides, such as  $\text{Cr}_2\text{O}_3$ ,  $\text{CaO}$ ,  $\text{MgO}$ , and  $\text{CeO}_2$ , cannot be laser melted at ambient pressure owing to high evaporation rates. Potentially, this could be bypassed by designing a high-pressure aerodynamic levitation chamber, but this has not been undertaken. Thermal gradient in the sample is another limitation of aerodynamic levitators. In aero-acoustic levitation [28], a sample is stabilised in a gas jet through the superposition of standing acoustic waves. This allows precise control of the sample position and unimpeded multibeam laser heating [29]. However, this complex and expensive setup has never been utilised on a beamline, and to the authors' knowledge, there is only one such instrument in operation at Telle's laboratory in Germany [30].

### **Temperature profiles, differential thermal analysis (DTA) and calorimetry**

Measurement of temperature profiles on heating or cooling of the sample is the oldest thermal analysis approach with which latent heat of melting was first discovered by Joseph Black in 1757 [31]. The cooling profiles recorded on laser-heated aerodynamically levitated samples can be used to estimate solidus and liquidus temperatures for samples unimpeded by possible reaction with the container and without atmosphere restriction. We successfully used this method to corroborate Calphad models for the Fe–Cr–Al–O system [32]. However, owing to the relatively small mass of levitating sample, thermal arrests or recalescence peaks may be difficult to detect when the heat effects are small and undercooling is insignificant, as in the case for YSZ [33].



Modern thermal analysis techniques for temperature below 1500°C rarely include analysis of the cooling traces, instead favouring DTA and differential scanning calorimetry (DSC) methods. DTA and DSC allow straightforward measurement of temperatures and enthalpies of transformation through the use of commercially available instruments and established calibration procedures. Optical DTA [34] was developed, which employed radiation thermometry to monitor the difference between the sample and the reference temperature, but this technique had shared the limitation of the container requirements and did not result in commercialisation.

DTA measurements to 2600°C were reported by Shevtchenko and Lopato [35] with a custom-built instrument employing solar heating. High-temperature thermal analyzers are commercially offered by Setaram, Netzsch and Linseis. These instruments are nominally limited to 2400°C, use W-Re alloy sensors, thermocouples, and W crucibles for analysis of oxide samples. However, until recently Al<sub>2</sub>O<sub>3</sub> (T<sub>m</sub> 2054°C) was the only standard for calibration of heat effects and temperature above 2000°C. The Setaram Setsys 2400 instrument has been in operation at the UC Davis Thermochemistry Laboratory for more than 10 years. It was customised to allow excursions to 2500°C with temperature monitoring by a spectropyrrometer (Figure 1). In order to obtain reasonably accurate measurements of heat effects and temperatures above the melting temperature of alumina, a standard close to the upper range of the instrument was needed. The melting temperature of Y<sub>2</sub>O<sub>3</sub> is constrained to 2439 ± 12°C by measurements in several laboratories [36]. It is believed to be independent of the atmosphere within reported uncertainty. We confirmed this by melting Y<sub>2</sub>O<sub>3</sub> in Ar and O<sub>2</sub> flows in an aerodynamic levitator and recording the cooling temperature profiles using a Chino 875-925 nm spectral band pyrometer and a FAR spectropyrrometer [37].

The heat of fusion of  $\text{Y}_2\text{O}_3$  was previously measured by only one research group in a custom-built boiling water drop calorimeter on samples tens of grams in weight and vacuum sealed in W crucibles. In order to perform independent measurements, the drop-andcatch (DnC) calorimeter (Figure 2) was designed at UC Davis and validated by measurements of the fusion enthalpy of  $\text{Al}_2\text{O}_3$  [38]. In DnC calorimetry, sample beads  $\sim 3$  mm in diameter are laser heated in a splittable nozzle aerodynamic levitator then dropped and caught in a calorimeter at room temperature. For  $\text{Y}_2\text{O}_3$ , the step in enthalpy corresponds to the sum of the pre-melting phase transformation and the enthalpy of fusion. The obtained value,  $119 \pm 10$  kJ/mol, is within the uncertainty of previously reported values and in agreement with results of ab initio molecular dynamic (AIMD) simulations [37]. The DnC technique was then employed for fusion enthalpy measurements of  $\text{ZrO}_2$ ,  $\text{HfO}_2$ ,  $\text{Lu}_2\text{O}_3$ , and  $\text{Yb}_2\text{O}_3$  (Table 1). The detailed reports are submitted for publication. Relatively high uncertainties in fusion enthalpy ( $\sim 10$  kJ/mol) from the DnC technique are owing to the large thermal gradients in the levitated sample. High-temperature heat capacity cannot be derived from DnC since it is not possible to accurately account for cooling during the drop. High-temperature DTA, when applicable, would provide higher accuracy. However, DnC calorimetry was found instrumental for measurements of fusion enthalpy on oxide compounds that react with the W crucible, and thus are unsuitable for DTA. Replacing the calorimeter plates with a solid copper block allows the use of the same instrument for splat quenching experiments. Another advantage of DnC is that experiments can be performed above  $2500^\circ\text{C}$ , with sample vaporisation being the only limiting factor.

### **X-ray and neutron diffraction on laser-heated levitated samples**

Due to the sample containment issues discussed above, high-temperature diffraction measurements on oxides above  $1800^\circ\text{C}$  were traditionally restricted to inert environments and

were limited by interaction with the container. Aerodynamic levitators on synchrotron sources, initially developed for melt studies and the possibility to use them for high-temperature X-ray diffraction on solid samples, have not been fully exploited until recently. Despite synchrotron XRD patterns from laser-heated levitated solids appearing in several publications devoted to the structure of melts, they were not used for refinement of thermal expansion, and escaped due attention from the ceramic community.

Our first use of the aerodynamic levitator at APS for X-ray diffraction on solids aimed to identify the high-temperature structure of  $Y_2O_3$  stable at  $100^\circ C$  below its melting temperature. There were conflicting reports in the literature whether  $Y_2O_3$  transforms into a defect fluorite structure before melting, or follows other lanthanide oxides, forming a disordered hexagonal phase [2]. The experimental setup for diffuse scattering measurements on melts included an amorphous silicon area detector in front of the aerodynamic levitator chamber and required no modification to obtain powder-like diffraction patterns for solid samples. Sample beads for levitation are usually prepared by laser melting and have cavities in the surface owing to a decrease in volume on crystallisation. This naturally occurring geometry promotes sample rotation in a gas flow, which is required to collect powder-like diffraction patterns from the solid crystalline sample. It is possible in most cases to induce the rotation of the solid beads by adjusting gas flow through the levitator nozzle.

The typical sample to detector distance used at APS for the collection of X-ray scattering data on melts is around 30 cm, which with X-ray energy of ca. 100 keV, provides a Q-space range of about  $25 \text{ \AA}^{-1}$ . It is possible to refine unit cell parameters from diffraction on solid phases in this configuration, however moving the detector to a 1-meter distance allows higher resolution in a lower angle range (Figure 3) usable for refinement. Dimensions and levitation

heights between beads may differ by hundreds of microns. Calibration of the sample position with respect to the beam and detector is more critical for cell parameters and thermal expansion refinements than for pair distribution function (PDF) analysis of melts, since Bragg peaks are much sharper than peaks for interatomic distances in melts. The developed best practice procedure includes calibration for every bead using the room temperature cell parameter before and after heating the sample. The conservatively estimated accuracy for cell parameters on levitating samples is  $\pm 0.003 \text{ \AA}$ . The systems studied by this technique are summarised in Table 2 with references to detailed reports. The utility of this method for solids exceeded by far our modest initial expectations of phase identification. Complete high-temperature structure refinements of several rare earth pyrochlores were performed providing antisite and vacancy occupancies as a function of temperature that allowed calculation of configurational entropies and defect energies [48,49]. Neutron diffraction on solid levitated samples was also successfully performed on the NOMAD instrument at the Spallation Neutron Source at Oak Ridge National Laboratory . This instrument has six operating detector banks (Figure 3), providing data for different d-spacing ranges, and no modification was needed to perform the experiments on solids. In addition to the thermal expansion, neutron diffraction data allowed refinement of thermal parameters for oxygen in YSZ and lanthanum zirconate using data from a single 67 degree scattering bank [33]. Powder-like synchrotron diffraction patterns from levitated beads  $\sim 3 \text{ mm}$  in diameter can be obtained in less than 1 s, compared to 10 min or more required for neutron diffraction data collection.

### **Summary and Future Development**

The methods described above allow us to obtain structural and thermodynamic data on oxides above  $2000^\circ\text{C}$  that can be used for input and validation of Calphad models and correlated with

DFT and AIMD computations. Simple recordings of the cooling traces on laser-melted levitated samples provide insights into melting behaviour, undercooling, phase transformation and atmospheric effects. Commercial DTA calibrated with  $\text{Al}_2\text{O}_3$ , and  $\text{Y}_2\text{O}_3$  melting temperatures and heats of fusion can provide data for oxides above  $2000^\circ\text{C}$ , but is limited to inert environments and by reactions with W crucibles. The recently developed DnC calorimetry technique allows the measurement of fusion enthalpies above  $2000^\circ\text{C}$  in variable atmospheres, and can be used for splat quenching. The main limitation of experimental approaches involving laser heating lies in uniaxial surface heating of levitated samples, causing thermal gradients of more than  $100^\circ\text{C}$  across the sample (spheroid, 2–3 mm in diameter), leading to uncertainties in fusion enthalpy values of as much as  $\pm 10$  kJ/mol and limiting the temperature resolution of diffraction data. Possible solutions to be explored and tested include multi-beam dual-laser heating and preheating of the levitation gas.

DnC calorimetry and in situ structural measurements on levitated samples provide new tools for basic and applied research on oxides above  $2000^\circ\text{C}$ . Areas where improvements in capabilities can add significant value and where further work is planned include (i) improved control of temperature gradients in samples; (ii) improved non-contact temperature measurement; (iii) operation at pressures above 1 bar. It is our hope that efforts in fundamental research on the high-temperature structures and thermodynamics of  $\text{ZrO}_2$ ,  $\text{HfO}_2$ , and rare earth oxides will help to establish triangulation pillars that can be used for navigation, by computational means, in the 100+ dimensional space of the periodic table in search of the right combinations of elements for materials for any application.

## **Acknowledgements**

Use of the Advanced Photon Source (APS, beamline 6-IDD), an Office of Science User Facility operated for the DOE Office of Science by Argonne National Laboratory, was supported by the DOE under Contract No. DEACO2-06CH11357. Development of the aerodynamic levitator for use at the synchrotron was supported by DOE Contract No. DE-SC0015241. The Spallation Neutron Source at Oak Ridge National Laboratory was supported by the Scientific User Facilities Division, Office of Basic Energy Sciences, US Department of Energy.

## **Funding**

This work was supported by the National Science Foundation Division of Materials Research [grant number 1506229 and 1835848].

Table 1. Fusion enthalpies for oxides and compounds studied above 2000°C by DTA and DnC calorimetry.

Composition	T <sub>m</sub> (°C)	$\Delta H_{\text{fus}}$ (kJ/mol)	Method [Ref]
HfO <sub>2</sub>	2800	61 ±10	DnC [39]
ZrO <sub>2</sub>	2710	55 ±7	DnC [39]
Y <sub>2</sub> O <sub>3</sub>	2439	119 ±10 <sup>a</sup>	DnC [37]
La <sub>2</sub> O <sub>3</sub>	2305	78 ±10	DTA [40]
Nd <sub>2</sub> O <sub>3</sub>	2308	117 ±10	DTA [41]
Yb <sub>2</sub> O <sub>3</sub>	2435	102 ±10	DnC [42]
Lu <sub>2</sub> O <sub>3</sub>	2490	125 ±10	DnC [42]
LaAlO <sub>3</sub>	2134	124 ±10	DTA [43]
La <sub>2</sub> Zr <sub>2</sub> O <sub>7</sub>	2260	300 ±50	DTA [44]

<sup>a</sup>includes the enthalpy of pre-melting (C-H) transition at 2327°C

Table 2. Oxides studied above 2000°C by X-ray and neutron diffraction on laser-heated aerodynamically levitated samples and their mean linear thermal expansion coefficients for the indicated temperature range.

Composition	<i>T</i> range (°C)	$\alpha$ ( $10^{-6} \text{ K}^{-1}$ )	Phase and experimental conditions <sup>a</sup>
HfO <sub>2</sub>	2530 - 2800	13 ±4	Flrt to Tm, XRD in O <sub>2</sub> [39]
ZrO <sub>2</sub>	2311 - 2710	12 ±3	Flrt to Tm, XRD in O <sub>2</sub> [39]
Y <sub>2</sub> O <sub>3</sub>	25 - 2327	9.3 ±0.1	C-type to T(C-H), XRD in O <sub>2</sub> [2]
Ho <sub>2</sub> O <sub>3</sub>	25 - 2185	8.1 ±0.1	C-type to T(C-B), XRD in O <sub>2</sub> [46]
Er <sub>2</sub> O <sub>3</sub>	25 - 2320	8.8 ±0.2	C-type to T(C-H), XRD in O <sub>2</sub> [46]
Yb <sub>2</sub> O <sub>3</sub>	25 - 2435	8.5 ±0.6	C-type to Tm, XRD in O <sub>2</sub> [47]
Lu <sub>2</sub> O <sub>3</sub>	25 - 2490	7.7 ±0.6	C-type to Tm, XRD in O <sub>2</sub> [47]
Zr <sub>0.9</sub> Y <sub>0.1</sub> O <sub>1.95</sub>	1600 – 2300 <sup>b</sup>	7.1 ±1.9	Flrt, ND in Ar [33]
Zr <sub>0.7</sub> Eu <sub>0.3</sub> O <sub>1.85</sub>	700-2100	10.7 ±0.4	Flrt, XRD in O <sub>2</sub> [48]
La <sub>2</sub> Zr <sub>2</sub> O <sub>7</sub>	1600 – 2300	7.5 ±1.0	Pyr to Tm, ND in Ar [33]
Eu <sub>2</sub> Zr <sub>2</sub> O <sub>7</sub>	700-2100	8.6 ±0.2	Pyr, Flrt above 1900°C, XRD in O <sub>2</sub> [48]
Nd <sub>2</sub> Zr <sub>2</sub> O <sub>7</sub>	850-2050	10.7 ±0.6	Pyr, XRD in O <sub>2</sub> [49]
Sm <sub>2</sub> Zr <sub>2</sub> O <sub>7</sub>	850-2050	10.9 ±0.4	Pyr, XRD in O <sub>2</sub> [49]
Gd <sub>2</sub> Zr <sub>2</sub> O <sub>7</sub>	850-2050	10.3 ±0.2	Pyr, Flrt above 1600°C, XRD in O <sub>2</sub> [49]
La <sub>2</sub> Hf <sub>2</sub> O <sub>7</sub>	850-2050	8.7 ±0.5	Pyr, XRD in O <sub>2</sub> [49]
Nd <sub>2</sub> Hf <sub>2</sub> O <sub>7</sub>	850-2050	9.9 ±0.5	Pyr, XRD in O <sub>2</sub> [49]
Sm <sub>2</sub> Hf <sub>2</sub> O <sub>7</sub>	850-2050	10.1 ±0.3	Pyr, XRD in O <sub>2</sub> [49]

<sup>a</sup>Phases abbreviations, singony, and space group (SG): Flrt – fluorite or defect fluorite, cubic (*Fm-3m*),

Pyr – pyrochlore, cubic (*Fd-3m*), C– bixbyite, cubic (*Ia-3*), B – monoclinic (*C2/m*), H – hexagonal

(*P63/mmc*); <sup>b</sup>25 · 10<sup>-6</sup> K<sup>-1</sup> above 2300°C.



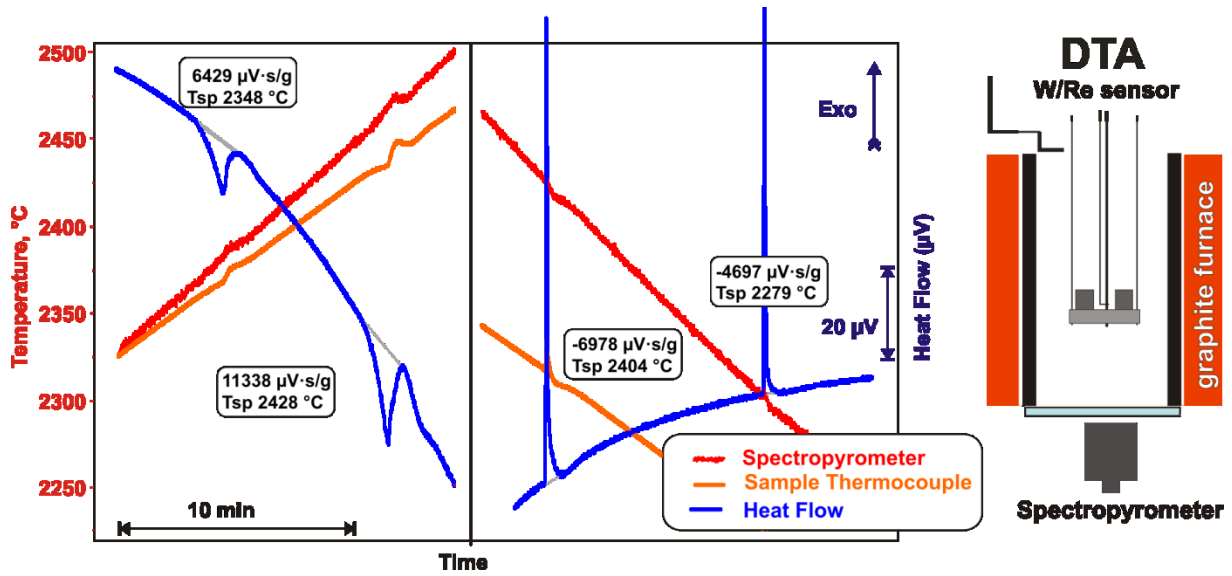


Figure 1. DTA of melting and crystallisation of  $Y_2O_3$  and instrument schematics. Experiments performed in Ar flow at  $10^{\circ}C/min$  heating and cooling rates on 87.34 mg  $Y_2O_3$ , laser melted and sealed in W crucible. No corrections or baseline subtractions applied. Cooling and heating segments were recorded with different sensors – note the difference between sample thermocouple and pyrometer readings as a function of temperature and between two sensors.

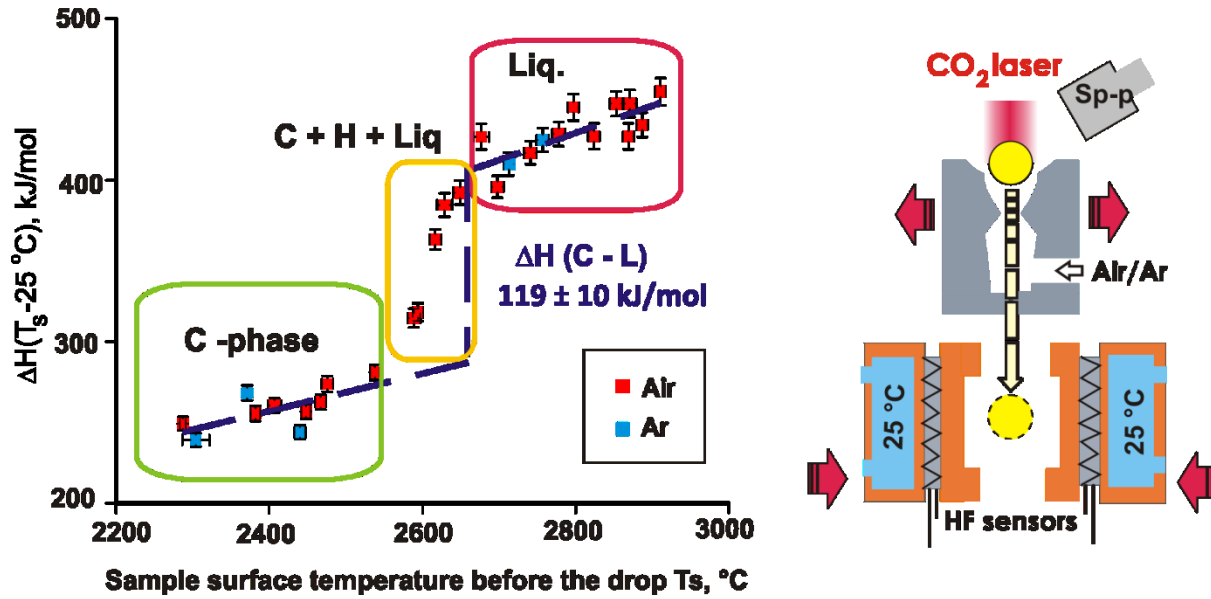


Figure 2. Enthalpy versus surface temperature plot from DnC calorimetry experiments on  $\text{Y}_2\text{O}_3$  [37] and instrument schematic. No distinct separation between cubic–hexagonal (C–H) pre-melting transition and melting could be observed owing to thermal gradient in the sample.

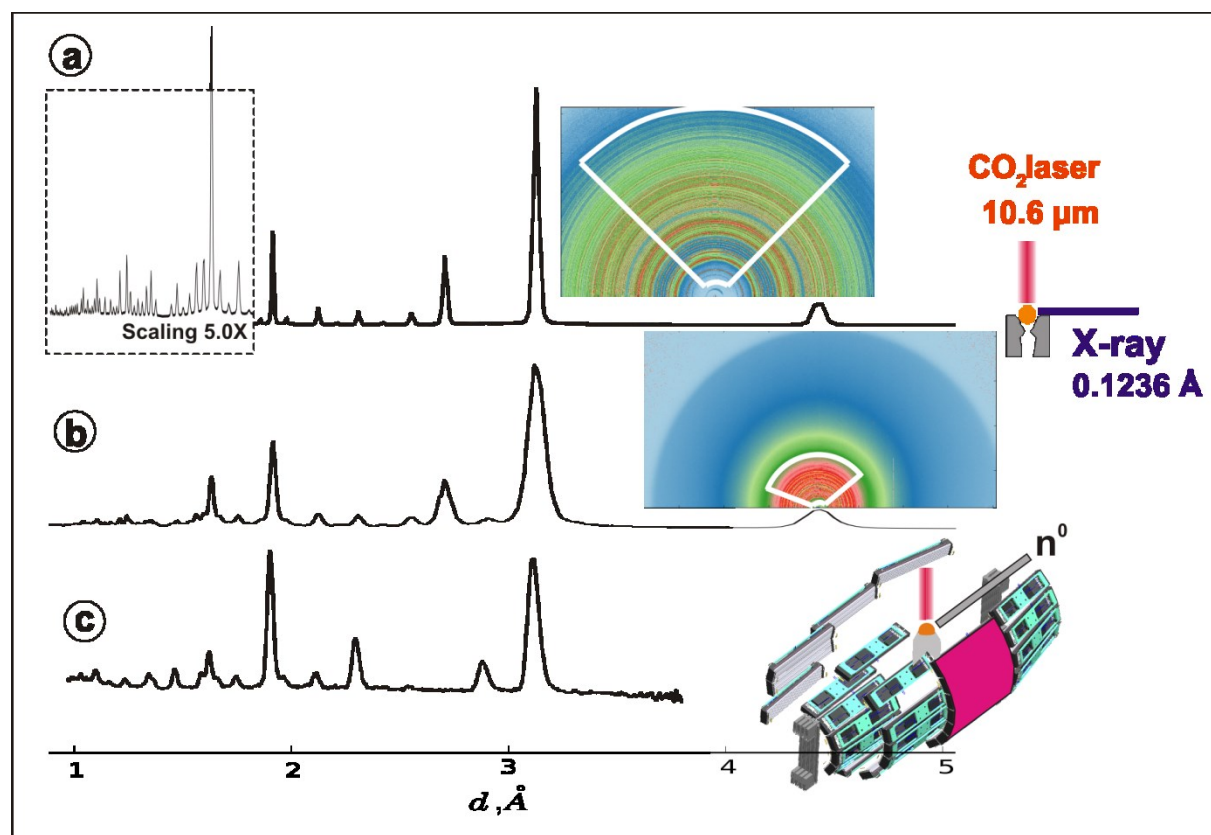


Figure 3. Synchrotron X-ray and time-of-flight neutron diffraction patterns of  $\text{Y}_2\text{O}_3$  at  $2000^\circ\text{C}$  collected on aerodynamically levitated laser-heated sample bead ( $\sim 3$  mm in diameter). (a) X-ray diffraction at 114 cm sample-to-detector distance, pattern obtained by integration of the selected sector of the diffraction image. Acquisition time 10 s ( $100 \times 0.1$  s exposures). (b) X-ray diffraction at 34 cm sample-to-detector distance. Acquisition time 12 s ( $120 \times 0.1$  s exposures). (c) Time-of-flight neutron diffraction pattern from 67 degree scattering bank of NOMAD instrument (selected on the instrument schematic). Acquisition time: 40 min. Intensities not to scale. GSAS-II [45] was used for integration and plots.

## References

1. Fahrenholtz WG, Wuchina EJ, Lee WE, et al. Ultra-high temperature ceramics: materials for extreme environment applications. Hoboken (NJ): Wiley; 2014.
2. Ushakov SV, Navrotsky A. Experimental approaches to the thermodynamics of ceramics above 1500°C. *J Am Ceram Soc.* 2012;95:1463-1482. doi: 10.1111/j.1551-2916.2012.05102.x.
3. McGrath JR. Exploding Wire Research 1774 - 1963. Naval Research Lab memorandum report 1698, accession number AD0633623, Washington, D.C. 1966.  
<http://www.dtic.mil/docs/citations/AD0633623>
4. Huepf T, Cagran C, Pottlacher G. Thermophysical properties of 22 pure metals in the solid and liquid state - the pulse-heating data collection. *EPJ Web Conf.* 2011;15:01018. doi: 10.1051/epjconf/20111501018.
5. Kaufman L, Ågren J. Calphad, first and second generation – birth of the materials genome. *Scr Mater.* 2014;70:3-6. doi: 10.1016/j.scriptamat.2012.12.003.
6. Luo AA. Material design and development: from classical thermodynamics to CALPHAD and ICME approaches. *Calphad.* 2015;50:6-22. doi: 10.1016/j.calphad.2015.04.002.
7. Wang C, Zinkevich M, Aldinger F. On the thermodynamic modeling of the Zr-O system. *CALPHAD: Comput Coupling Phase Diagrams Thermochem.* 2004;28(3):281-292. doi: 10.1016/j.calphad.2005.09.002.
8. Kelley KK. Contributions to the data on theoretical metallurgy. V. Heats of fusion of inorganic substances. *Bur Mines, Bull.* 1936;No. 393:166.

9. DeWitt DP, Nutter G.D. Theory and practice of radiation thermometry. New York: Wiley; 1988.
10. Hyde EP, Forsythe WE. The visibility of radiation in the red end of the visible spectrum. *Astrophys J.* 1915;42:285-93. doi: 10.1086/142207.
11. Langmuir I. The melting-point of tungsten. *Physical Rev.* 1915;6(2):138-157.
12. Razor NS, McClelland JD. Thermal property measurements at very high temperatures. *Rev Sci Instrum.* 1960;31:595-604. doi: 10.1063/1.1931263.
13. Stein A, Rabinowitz P, Kaldor A, inventors; Exxon Research and Engineering Company, assignee. Laser radiometer patent US4417822 (A). 1983.
14. Felice RA, inventor. Temperature determining device and process patent US5772323 (A). 2002.
15. Felice RA. The spectropyrometer - a practical multi-wavelength pyrometer. *AIP Conf Proc.* 2003;684(2):711-716.
16. Lu H, Ip LT, Mackrory A, et al. Particle surface temperature measurements with multicolor band pyrometry. *AIChE Journal.* 2009;55(1):243-255. doi: 10.1002/aic.11677.
17. Earl DD, Kisner RA, Earl DD, et al., inventors; UT-BATTELLE, LLC; UT-Battelle, LLC, assignee. Emissivity Independent Optical Pyrometer patent US2015124244 (A1). 2017.
18. Benezech G, Berjoan R, Coutures JP, et al. Thermal analytical apparatus for the study of crystalline transformations and phase changes at high temperature. *Colloq Int Cent Nat Rech Sci.* 1972;205:57-69.

19. Manara D, Sheindlin M, Heinz W, et al. New techniques for high-temperature melting measurements in volatile refractory materials via laser surface heating. *Rev Sci Instrum.* 2008;79:113901/1-113901/7. doi: 10.1063/1.3005994.
20. Jackson HF, Jayaseelan DD, Manara D, et al. Laser melting of zirconium carbide: determination of phase transitions in refractory ceramic systems. *J Am Ceram Soc.* 2011;94:3561-3569. doi: 10.1111/j.1551-2916.2011.04560.x.
21. Winborne DA, Nordine PC, Rosner DE, et al. Aerodynamic levitation technique for containerless high temperature studies on liquid and solid samples. *Metall Trans, B.* 1976;7:711-13. doi: 10.1007/bf02698607.
22. Nordine PC, Atkins RM. Aerodynamic levitation of laser-heated solids in gas jets. *Rev of Sci Instrum.* 1982;53(9):1456-1464. doi: 10.1063/1.1137196.
23. Krishnan S, Felten JJ, Rix JE, et al. Levitation apparatus for structural studies of high temperature liquids using synchrotron radiation. *Rev Sci Instrum.* 1997;68(9):3512-3518. doi:10.1063/1.1148315
24. Kurisuchiyan B, Jiyan PK, Dominiku M, et al., inventors; Sadis Bruker Spectrospin, assignee. Probe for Spectroscopic Measurement of Magnetic Resonance at Super High Temperature patent JPH0210281 (A). 1990.
25. Benmore CJ, Weber JKR. Aerodynamic levitation, supercooled liquids and glass formation. *Adv in Phys: X.* 2017;2(3):717-736. doi: 10.1080/23746149.2017.1357498.
26. Hennet L, Cristiglio V, Kozaily J, et al. Aerodynamic levitation and laser heating. *Eur Phys J Spec Top.* 2011;196(1):151-165. doi: 10.1140/epjst/e2011-01425-0.
27. Hennet L, Moritz DH, Weber R, et al. Chapter 10 - high-temperature levitated materials. In: Fernandez-Alonso F, Price DL, editors. *Experimental methods in the physical*

- sciences. Vol. 49. Amsterdam: Academic Press; 2017. p. 583-636. doi:10.1016/B978-0-12-805324-9.00010-8
28. Nordine PC, Weber JKR, Abadie JG. Properties of high-temperature melts using levitation. *Pure Appl Chem.* 2000;72(11):2127-2136. doi: 10.1351/pac200072112127.
  29. Nordine PC, Merkley D, Sickel J, et al. A levitation instrument for containerless study of molten materials. *Rev Sci Instrum.* 2012;83(12):125107/1-125107/14. doi: 10.1063/1.4770125.
  30. Telle R, Greffrath F, Prieler R. Direct observation of the liquid miscibility gap in the zirconia-silica system. *J Eur Ceram Soc.* 2015;35(14):3995-4004. doi: 10.1016/j.jeurceramsoc.2015.07.015.
  31. Bent HA. *The second law: an introduction to classical and statistical thermodynamics.* New York: Oxford University Press; 1965.
  32. McMurray JW, Hu R, Ushakov SV, et al. Solid-liquid phase equilibria of Fe-Cr-Al alloys and spinels. *J Nucl Mater.* 2017;492:128-133. doi: 10.1016/j.jnucmat.2017.05.016.
  33. Ushakov SV, Navrotsky A, Weber RJK, et al. Structure and thermal expansion of YSZ and  $\text{La}_2\text{Zr}_2\text{O}_7$  above 1500°C from neutron diffraction on levitated samples. *J Am Ceram Soc.* 2015;98(10):3381-3388. doi: 10.1111/jace.13767.
  34. Caslavsky JL. Principles of the optical differential thermal analysis (ODTA). *Thermochim Acta.* 1988;134:371-6. doi: 10.1016/0040-6031(88)85262-6.
  35. Shevchenko AV, Lopato LM. TA method application to the highest refractory oxide systems investigation. *Thermochim Acta.* 1985;93:537-40.
  36. Hlavac J. Melting temperatures of refractory oxides. part I. *Pure Appl Chem.* 1982;54:681-8. doi: 10.1351/pac198254030681.

37. Kapush D, Ushakov S, Navrotsky A, et al. A combined experimental and theoretical study of enthalpy of phase transition and fusion of yttria above 2000° C using “drop-n-catch” calorimetry and first-principles calculation. *Acta Mater.* 2017;124:204-209. doi:10.1016/j.actamat.2016.11.003
38. Ushakov SV, Shvarev A, Alexeev T, et al. Drop-and-catch (DnC) calorimetry using aerodynamic levitation and laser heating. *J Am Ceram Soc.* 2017;100(2):754-760. doi: 10.1111/jace.14594.
39. Hong Q-J, Ushakov SV, Kapush D, et al. Combined computational and experimental investigation of high temperature thermodynamics and structure of cubic ZrO<sub>2</sub> and HfO<sub>2</sub>. *Sci Rep.*, submitted, 2018.
40. Ushakov SV, Navrotsky A. Direct measurements of fusion and phase transition enthalpies in lanthanum oxide. *J Mater Res.* 2011;26:845-847. doi: 10.1557/jmr.2010.79.
41. Navrotsky A, Ushakov SV. Hot matters - experimental methods for high-temperature property measurement. *Am Ceram Soc Bull.* 2017;96(2):22-28.
42. Fyhrie M, Hong Q-J, Kapush D, et al. Energetics of melting of Yb<sub>2</sub>O<sub>3</sub> and Lu<sub>2</sub>O<sub>3</sub> from Drop and Catch Calorimetry and First Principles Computations, *J Chem Thermo*, submitted, 2018.
43. Ushakov SV, Navrotsky A. Direct measurement of fusion enthalpy of LaAlO<sub>3</sub> and comparison of energetics of melt, glass, and amorphous thin films. *J Am Ceram Soc.* 2014;97(5):1589-1594.
44. Radha AV, Ushakov SV, Navrotsky A. Thermochemistry of lanthanum zirconate pyrochlore. *J Mater Res.* 2009;24:3350-3357. doi: 10.1557/jmr.2009.0401.



45. Toby BH, Von Dreele RB. GSAS-II: the genesis of a modern open-source all purpose crystallography software package. *J Appl Crystallogr.* 2013;46(2):544-549. doi: 10.1107/S0021889813003531.
46. Ushakov SV, Pavlik A, Hong Q-J, et al. in preparation. 2018.
47. Pavlik A, Ushakov SV, Navrotsky A, et al. Structure and thermal expansion of  $\text{Lu}_2\text{O}_3$  and  $\text{Yb}_2\text{O}_3$  up to the melting points. *J Nucl Mater.* 2017;495(Suppl. C):385-391. doi: 10.1016/j.jnucmat.2017.08.031.
48. Maram PS, Ushakov SV, Weber RJK, et al. In situ diffraction from levitated solids under extreme conditions-structure and thermal expansion in the  $\text{Eu}_2\text{O}_3$ - $\text{ZrO}_2$  system. *J Am Ceram Soc.* 2015;98(4):1292-1299. doi: 10.1111/jace.13422.
49. Maram PS, Ushakov SV, Weber JKR, et al. Probing disorder in pyrochlore oxides using in situ synchrotron diffraction from levitated solids – A thermodynamic perspective *Sci Rep.* 2018;8:10658.